

Thermal simulation of the Effect of Windings Arrangement in a Cooled Power Transformer

¹ALEJANDRO ROBERTO TELLO CAMPOS, ¹WILLIAM VICENTE RODRÍGUEZ, ¹JOSÉ LUIS FERNÁNDEZ ZAYAS

¹Instituto de Ingeniería
Universidad Nacional Autónoma de México
Cd. Universitaria, 04510, México D.F.

¹ AtelloC@iingen.unam.mx, ¹WV@iingen.unam.mx, ¹joseluis.fernandez@iie.org.mx

²IGNACIO CARVAJAL MARISCAL

² Instituto Politécnico Nacional
Laboratorio de Térmica e Hidráulica Aplicadas
Av. IPN s/n Edif.5, 3er Piso, 07738, México D.F.
² icarvajal@ipn.mx

³RODRIGO OCON VALDEZ

³Industrias IEM S.A de C.V. Vía Dr. Gustavo Baz No. 340,
Tlalnepantla Edo. De México CP 54000.

Abstract: The outcome of the study will be the determination of the effects of modifying geometrical parameters of a real 33.6 MVA power transformer by means of a simplified model based on CFD methods. This will help the designers to prove that power transformers winding physical arrangements determine the location and value of critical temperatures such as the hot spot. Basically, the results show that a the proposed variations in the outer radius of the high voltage winding and the high and low voltage vertical cooling duct widths do affect the critical temperatures location and value due to oil hydrodynamics. Results show that there is a reduction of 3.21% and 1.34% in the value of critical temperatures for the HV and LV cooling duct variation respectively and the location of hot spot is more specifically defined at the 42th LV disc. Outer HV radius variation results show also an increase of 1.6% in critical temperature and the location of hot spot still remains in the 42th LV disc.

Keywords: Power transformer, mixed convection, CFD, thermal simulation, geometrical parameters

1. Introduction

The industry of transformers continues working on the improvement of the cooling system of high capacity transformers. Transformers as such are key part of every industry. They transform the energy from one level of voltage to another. Those levels are specific and the low voltage range is from 220/440 V to 34/69 kV in the medium range and above 69 kV in the high voltage range. These devices normally operate under a variety of loading conditions. They are composed of high/low voltage windings which along with a central core are contained in a tank filled with mineral oil. To complete the design a set of radiators are attached in order to improve the heat dissipation. Also, they have other electrical parts which facilitate the electrical process. They can operate from under normal nominal load to above normal nominal load. Then the inner parts of the transformer such as the high/low voltage windings and isolators are subjected to relatively high temperatures which in time cause a failure. In this regard many researchers have defined several thermal models in order to predict the hot spot in the windings (the point of maximum temperature). One of the most popular ones are the thermal-hydraulic models networks developed on the basis of being able to predict the pressures and temperatures in concentrated nodes which are previously defined by the researcher[4]. These models have proved to be very efficient in the determination of temperatures and pressures of cooling oil in ducts. Another type of model refers to the use of CFD to define accurately the temperatures in windings and cooling oil. In this sense these models rely on the solution of the mass and momentum equations along with the energy equation. These equations are discretized and solved using efficient algorithms [1,2,3,7]. These models provide valuable information in terms of detailed temperature fields in the windings and cooling oil of foil type power transformers. They have been used also to provide the location of

hot spot as well as the nature of the oil dynamics within the ducts and at other points of interest within the transformer. Although these models have been used to study temperature and velocity distributions in power transformers their application has been limited to relatively simple winding geometries as a number of blocks representing discs in an LV winding. Other authors who have used CFD are more interested in the design of the cooling system composed by the radiators [5]. In this respect the authors analyze the effect of cooling in reference to the thermal efficiency of the radiators of a distribution transformer. Moreover, other researchers[8] have investigated the influence of some parameters such as the inlet temperature profile and oil mass flowrate on the value and location of the hot spot in disc type windings. Additionally some researchers [9] have developed mathematical models to predict the value and location of the hotspot within power transformers. In the IEEE standards [6] only provide the average oil temperature, winding temperature and hot spot based on a methodology which has been proved over the years. Manufacturers use rules of thumb in order to calculate the thermal load that a radiator has to dissipate and define the number of sections and oil cooling ducts that are required. These rules come from empirical data used to derive them. Experimental work requires precise and complex intrusive measurements which are difficult to obtain and can be made only in specific places within the geometry of a real transformer.

This paper proposes to develop a CFD model for a columns type power transformer which will help to determine the influence of windings-core arrangement on the location of the critical temperatures and the effect of the cooling of the windings. In this regard a variation in the HV and LV windings outer radius and in the HV and LV cooling duct width are proposed. This will give a detailed temperature and flow data in windings and cooling circuit. The model used considers the ONAN type of cooling in which oil circulates in a natural way within the transformer

and cooling equipment and air circulates in the outside of the radiator. A validation of the model is performed with thermal data (heat run test) provided by a local manufacturer.

Nomenclature:

c_p : Specific heat (J/kg K)
 E: energy (J/kg)
 g: Gravity acceleration ($=9.8 \text{ m/s}^2$)
 k: Thermal conductivity(W/m K)
 P: pressure (Pa)
 S: source term (W/m^3)
 T: temperature ($^{\circ}\text{C}$ or K)
 U: velocity component (m/s)

Abbreviations:

HV: high voltage
 LV: low voltage

Greek symbols:

ρ : density of oil(kg/m^3)
 Δ : difference
 β : expansion coefficient of oil (K^{-1})
 μ : absolute viscosity of oil ($Pa \cdot s$)

2. Power transformer considered for the study

The transformer to be considered for the analysis is shown in Fig. 1. This is a 33.6 MVA 115/34.5 kV three phase power transformer.



Fig. 1 The power transformer considered

A cross-section of the HV and LV windings, core, isolators and radiator of the power transformer is depicted in Fig. 2. The transformer considered is a columns type transformer which comprises a magnetic core surrounded by cylindrical disk type coaxial windings. The discs can be separated by oil guides but in this type there are only axial cooling ducts in order to direct the cooling oil. Each phase of the transformer is comprised of a high voltage winding (HV), a low voltage winding (LV), regulating windings, core, isolators, collars and supporting structures. The high voltage winding is composed of 45 discs (each composed of several copper conductors surrounded by paper as a dielectric isolator). The low voltage winding is composed of 43 discs. These windings, core, cardboard isolators and structures assembly are filled in cooling oil and contained in a steel tank. Oil circulates from bottom to top through vertical cooling ducts located among the windings. A flat plates radiator is provided in order to cool down the circulating oil coming from the windings and core assembly.

3. Power transformer CFD model

The proposed 2D CFD model is based on an axis-symmetric section of the windings-core-tank construction of the power transformer with the radiator section shown in Fig. 2.

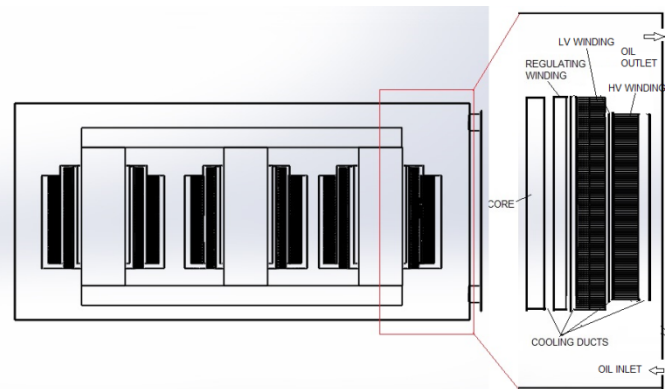


Fig. 2 Windings-core-tank construction

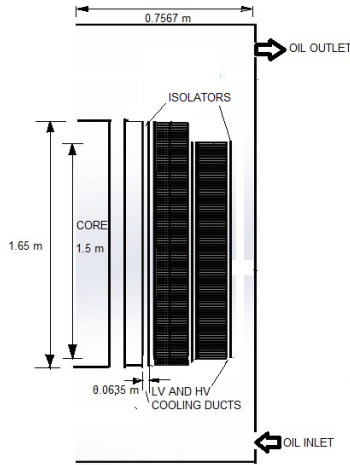


Fig. 3 Dimensions of the lv/hv windings

The 2D CFD model includes the discs type windings assembly construction. The dimensions of the low voltage and high voltage windings, tank and vertical cooling ducts are shown in Fig. 3.

Figure 4 depicts the dimensions of the cooling ducts considered as well as the height and width of the discs for the HV and LV winding.

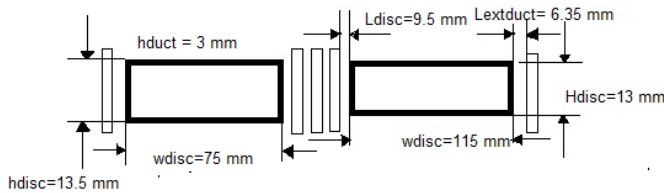


Figure 4 Dimensions of HV and LV discs

The 2D CFD discs type model considered herein is a simplified model due to the complexity of the geometry of the internal parts of the transformer. In this regard, the windings are composed of discs. These discs are composed of copper only. The insulation of each copper conductor and collar structures were not considered. In addition, only the isolation structures between windings as well as the corresponding section of the iron were considered.

Other assumptions and simplifications for this

CFD discs type model are as follows:

a) The ONAF (oil natural air forced) cooling type operates with a cooling system composed of a radiator which provides an efficient outer cooling system. The case analyzed does not consider the radiator itself. Only the temperature and velocity of the cold oil are defined as an input to the CFD discs type model.

b) The heat losses from windings and iron are considered as constant. The losses were distributed evenly in the discs. The internal construction of the disc related to the conductors surrounded by paper was not considered. The heat convection coefficient is considered in the calculation based on the following equation for the disc assembly:

$$h = \frac{q}{T_{oil} - T_{solid}} \quad (1)$$

c) Walls including the lid and base are considered as adiabatic for the CFD disc type model.

4. Governing equations

The governing equations are the ones, which are considered for mass momentum and energy for the steady state of the fluid of the transformer as follows:

$$\nabla \cdot (\rho U) = 0 \quad (2)$$

$$\nabla \cdot (\rho U \times U) = -\nabla p + \mu(\nabla^2 U) + \rho g \beta (\Delta T) \quad (3)$$

$$\nabla \cdot (\rho c_p U T) = \nabla \cdot (k \nabla T) + S_E \quad (4)$$

The source term S can be replaced by the losses of the windings Q .

In order to take into account for the density change in the case of mixed convection, the Boussinesq model was used as follows:

$$\rho = \rho_0(1 - \beta\Delta T) \quad (5)$$

The solid interaction is included by solving the following heat conduction equation:

$$k \left[\left(\frac{\partial^2 T}{\partial x^2} \right) + \left(\frac{\partial^2 T}{\partial y^2} \right) \right] = S \quad (6)$$

The model considered was implemented in the Phoenix Code which is a CFD code based on the solution of the finite volume scheme using the algorithm proposed by Patankar [10]. The mass, momentum and energy are solved along with the Boussinesq approximation for density. The properties of the oil were considered to vary with temperature and a prescription was specified as follows [7]:

$$\rho(T) = 1098.72 - 0.72 T \quad (7)$$

$$k(T) = 0.1509 - 7.101E - 05T \quad (8)$$

$$c_p(T) = 807.163 + 3.58T \quad (9)$$

$$\mu(T) = 0.08467 - 0.0004T + 5E - 7T^2 \quad (10)$$

The boundary conditions for the case considered were adiabatic for the upper and bottom walls (lid and base) and the lateral wall. The heat sources represented by the windings and core were considered as constant and the detail is given in the following Table 1.

Table 1
Boundary conditions

| | |
|------------------------------|----------------------------|
| Core loss | 14500W |
| HV loss(3 Phases) | 67300 W, 22433 W/per phase |
| LV loss (3 Phases) | 75510 W, 25170 W/per phase |
| Regulating winding(3 phases) | 1813 W per phase |
| Tank (lateral wall) | adiabatic |
| Upper and lower walls | adiabatic |
| Inlet oil temperature | 320 K |
| Inlet oil velocity | 0.002 m/s |
| Outlet pressure | 0 kPa |

The isolators and discs used have a thermal conductivity of 0.04 W/m K, 383 W/m K respectively. The inlet velocity was taken in reference to the measurements found by other researchers in the case of mixed convection in disc type windings of a power transformer [7].

The grid used was composed of 98,400 cells at the beginning. Finally, the independence of the grid test was made. It was used 150,766 cells to test the independence of the grid for the solutions obtained.

5. Heat run test

A heat run test of a real 33.6 MVA power transformer was performed at the power transformers factory. This test is done in order to verify the calculated oil and windings temperature rises. It is designed to verify possible hot spots inside or outside windings of the transformer. The values obtained from the test are compared to the values of the CFD calculations. In this test a set of fiber optic probes were set as shown in Fig. 5. The physical setting of the probes is shown in Fig. 6. No account was taken regarding the variation of radial winding temperatures and only the probes were set at the most probable highest temperature in the winding.

The heat run test was performed for ONAN (oil natural, air natural) and ONAF (oil natural, air forced) cooling modes. The purpose of the heat run test is to verify the thermal capability of transformer. It is made using short circuit loading method whereby one winding is short circuited and sufficient current is circulated in the windings to generate a loss equivalent to the core loss plus load loss. The transformer is connected at its maximums loss position. Thermocouples are used to monitor the top oil temperature in the transformer and the air ambient temperature. The transformer is operated at this loading until the increase in oil

temperature over ambient does not change more than 2.5% or 1 °C in three hours. It can take up to 12 hr for temperature stabilization. Additional to normal test instrumentation, a fiber optical monitor was installed in order to monitor winding temperatures. Gallium Arsenide – GaAs (SCBG) technology (OTG series optical sensor) were used. These sensors have dimension of 0.170 mm OD, offering a fast response time of less than 10ms; with an accuracy of ± 0.3°C and resolution of 0.05°C.

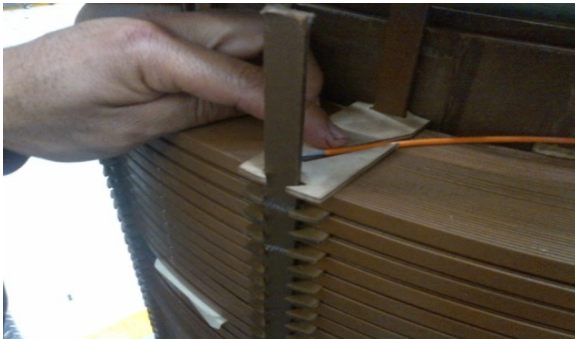


Fig. 5 Setting of the optic fiber probes

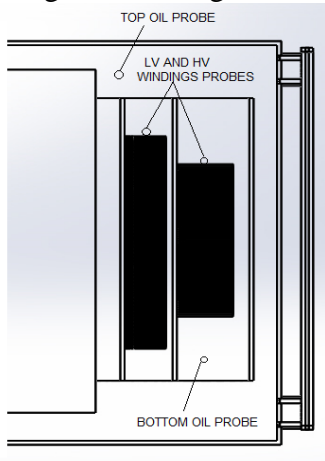


Fig.6 Location of probes

The temperatures of windings and oil obtained by means of the probes are shown in Table 2.

Table 2
Temperature measurements

| Probe position | Winding Temperature | Oil temperature |
|-----------------------|---------------------|-----------------|
| Upper part HV winding | 82.2°C(average) | 69°C (average) |
| Upper part LV winding | 101°C(average) | 69°C (average) |
| Lower part HV winding | 53°C (average) | 43°C(average) |
| Lower part LV winding | 53°C (average) | 43°C (average) |

6. Numerical results

The numerical results obtained are for the basic case which includes the windings-core-tank construction for the 2D CFD model . In this regard, a detailed temperature distribution can be shown in Fig. 7.

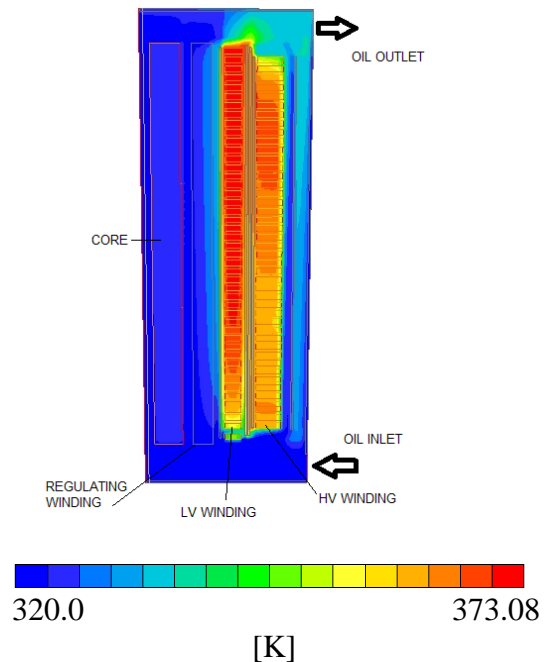


Fig. 7 Temperature contour

This Fig. 7 shows that HV winding temperature varies in the discs with regions of 89 °C (362 K) temperature and regions of 76 °C (349 K) at the discs located at the bottom of the winding. There is a region of high temperature of 114°C (387 K) in the LV winding. The LV winding temperature at the last upper disc is 106 °C (379 K).

Fig. 8 shows the centerline temperature of LV and HV oil cooling ducts and HV and LV windings as a function of the number of discs. These locations are critical regarding the hot spot in windings. Oil temperature increases with winding height which is a normal behavior for this kind of cooling in power transformers due to the thermosyphonic effect and flow provided at the inlet.. The HV winding temperature increases also with winding height and reaches the highest of 80 °C (353 K). The HV winding temperature varies along the winding height with some low and high values that are a result of the movement of oil at a low temperature of 47 °C (320 K) in an upward direction in the HV outer cooling duct. The LV winding temperature increases with height from 79 °C (352 K) to 100 °C (373 K).

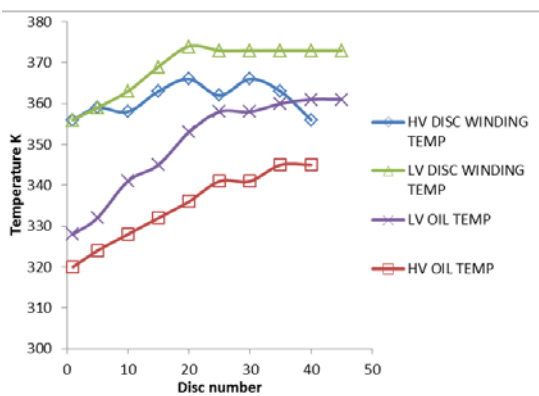


Fig. 8 Centerline temperatures

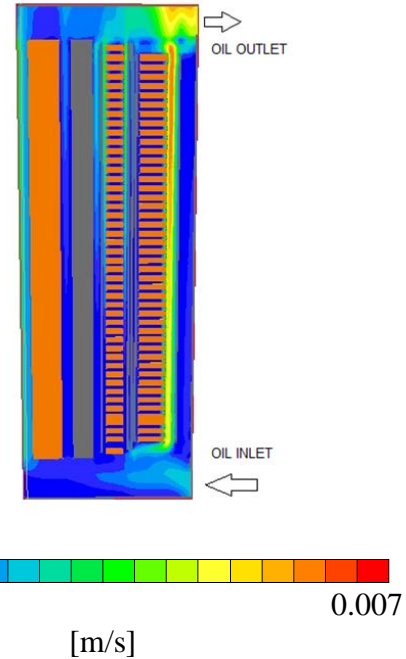


Fig. 9 Velocity contour

From Fig. 9 it can be observed that oil passes through the HV and LV winding sections at relatively low velocity. In the case of the LV winding the oil velocity decreases as it passes through the LV vertical cooling duct. It seems that the buoyancy force combined with pressure from inlet oil provides enough pressure to move more rapidly oil through the outer HV winding cooling duct, taking away more heat from the discs and providing a rather more efficient cooling. In the LV discs section oil accelerates at the beginning but then it decelerates and the discs in this case are not so efficiently cooled. In other vertical oil ducts near the core and the regulating winding oil accelerates but at a slower velocity and continues moving upwards at low velocity.

The Rayleigh number calculated based on the distribution of temperatures found in the detailed model shown in Fig. 7 was 1.64×10^6 for the high voltage winding and 7.5×10^5 for the low voltage winding. The Reynolds number based on the vertical cooling ducts width found was 8.58 which correspond to the laminar flow of oil.

When analyzing the numerical results obtained for the temperature of windings and oil in the CFD model it was found regions of high and low temperatures which clearly identify the critical zones. These values were compared to values found in the literature [11] and were found very consistent with the temperature distributions obtained when using FEM methods.

Table 3 shows a comparison of the temperatures found for the CFD disc type model and the heat run test.

Table 3

Comparison of windings and oil temperatures

| Temp. K | CFD model K | Heat run test K | % error (exp) |
|------------|-------------|-----------------|---------------|
| LV winding | 373 | 374 | 0.26 |
| LV oil | 341 | 342 | 0.29 |

Basically, the CFD model compared well with the reported values from the heat run test. The heat run test only provided with a point of high temperature located at the upper disc of the low voltage and high voltage winding and clearly no account was taken regarding the variation in temperature in the axial direction of the windings. The CFD model required 2000 iterations and the solution run time was about 2 h and 20 min. The mesh independency test was performed with a mesh 1.5 times larger than the original. The mean and maximum temperatures in discs showed a variation of approximately 1%. It shows that the hot spot found at the LV winding with the numerical study differs in 0.26% from the experimental value.

6.1 Variation in windings outer radius

As mentioned at the beginning an investigation of the effect of the vertical cooling duct was performed by varying the outer HV winding radius from 0.11588 m (4.5625 inches) to

0.135875 m. (5.3494 inches) This value of increase was considered based on an outer radius increase which could be done during the electrical design of the power transformer. The corresponding temperature contour is shown in Fig. 10.

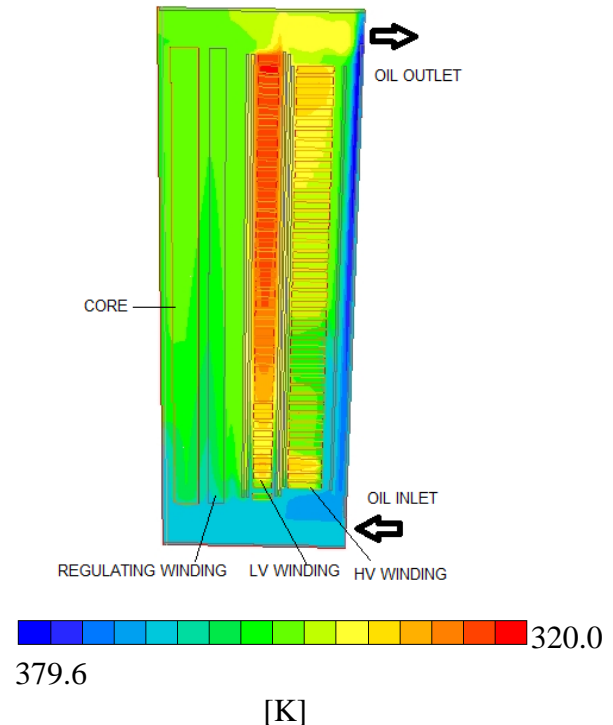


Fig. 10 Temperature contour

From Fig. 10 a clear reduction in windings temperature is shown. This increase in HV winding outer radius shows that the location of the region of high temperature (hot spot) varies from the top disc of the LV winding to the last top discs of the HV winding. The variation in LV winding temperature varies between 53°C (326 K) to 106 °C(379 K) at the bottom and top of the winding respectively. Regarding the HV winding the temperature varies between 67 °C (340 K) to 81 °C (354 K) at the top and bottom of the winding. The hot spot value predicted of 106°C (379 K) is increased because the HV winding heat dissipation is increased and the oil circulation is modified for the HV and LV windings. Comparing to the previous basic CFD model, the increase in hot spot was of the order of 0.79 %.

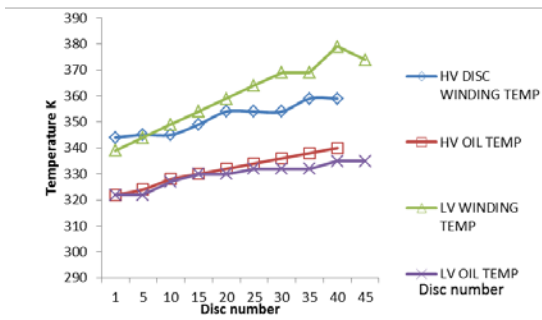


Fig. 11 Centerline temperatures

Fig. 11 shows that oil temperature increases steadily along the vertical coordinate while windings temperature has some striking differences. Regarding HV winding temperature it is found that it increases from 63 °C (336 K) to 76 °C (349 K) while LV winding temperature increase from 52 °C (325 K) to 73 °C (346 K). It is found that the first disc in the HV winding is at a temperature of 63 °C (336 K), then in the next discs temperature increases to a value of 76 °C (349 K) and continue to increase steadily up to the value of 86 °C (359 K). This behavior of temperature is due to the fact that although the HV windings outer radius was increased cooler oil reaches the HV and LV windings and heat transfer varies according to the oil temperature. On the contrary LV winding temperature increases steadily from 66 °C (339 K) to 106 °C (379 K) and at the last disc it decreases to 101 °C (374 K). Oil temperature in the HV oil cooling duct increases steadily from 47 °C (320 K) to 62 °C (335 K) while in the LV oil cooling duct increases almost in the same manner. Basically, cooler oil is redistributed between the HV and LV windings and the highest winding temperature increases.

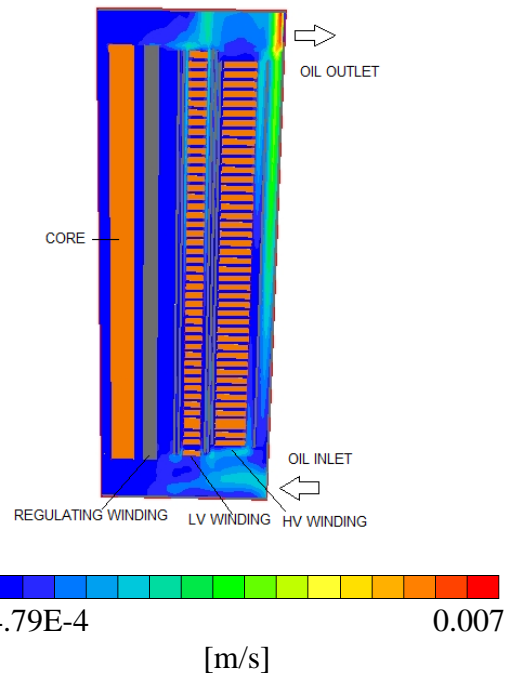


Fig. 12 Velocity contour

Velocities contour is shown in Fig. 12 for the case of the variation in HV outer radius. These figures show regions of low velocities through the windings sections and a relatively high velocity of the order of 0.001 to 0.003 m/s at the outer HV vertical cooling oil duct, inner and outer LV vertical cooling duct and regulating winding vertical cooling duct. The buoyancy force and pressure derived from the oil at the inlet in work more effectively to accelerate the oil which helps to reduce the HV winding temperature

6. 2 Variation in outer HV and LV vertical cooling duct width

Also, in a similar way another geometric factor was investigated regarding a variation in width of the HV cooling duct from 6.35 mm to 12.7 mm. Fig. 13 shows the corresponding temperature contour.

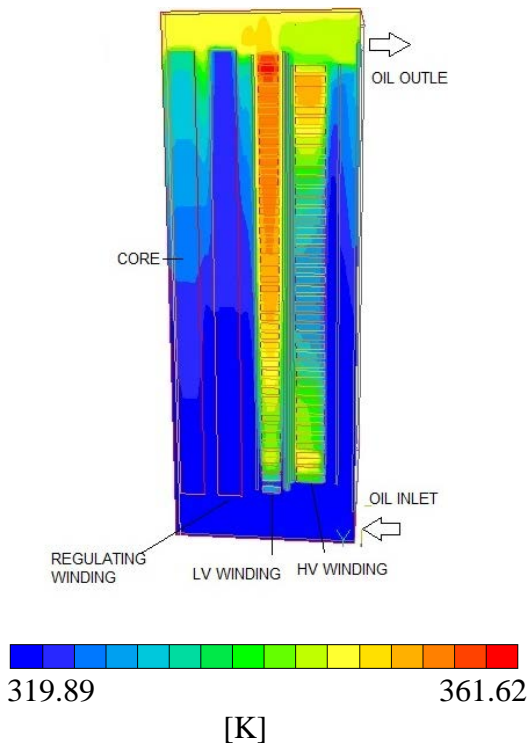


Fig. 13 Temperature contour

HV winding temperature shown on Figure 13 is increasing up to a value of 67 °C (340 K) at disc 16 and then it starts to drop to 57 °C (330 K) between discs 17 to 35 and continue increasing to a value of 79 °C (352 K). This trend is due to the fact that more cold oil is circulating upwards at 49 °C (322 K) and through the horizontal ducts at 54 °C (327 K) is reaching the discs 1 to 35 more effectively.

Fig. 14 shows a graph of the winding and oil temperature along the vertical centerline of the HV and LV windings and cooling ducts. As expected the LV winding temperature increases with height and the maximum 88 °C (361 K) is observed almost at the top of the winding.

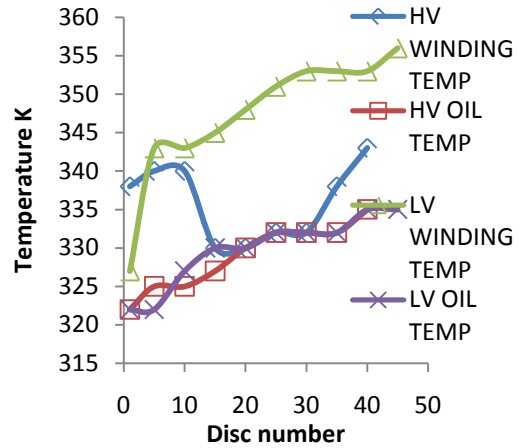


Fig. 14 Centerline temperatures

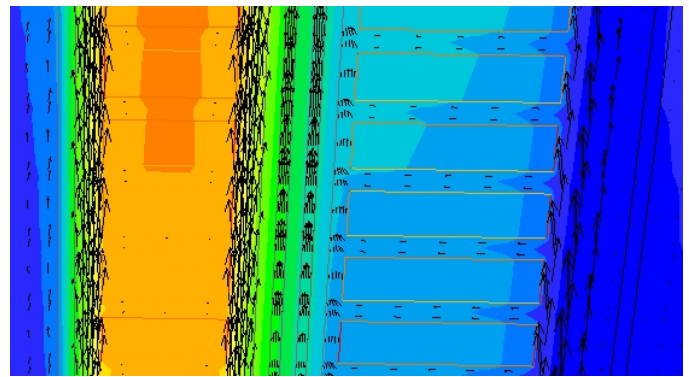


Fig. 15 Temperature close-up

A close up of Fig.13 is shown in Fig. 15. It shows that some cold oil at 49 °C (322 K) from the outer HV cooling duct as previously mentioned enters the horizontal cooling ducts and mixes with oil at 57 °C (330 K). Then the HV discs temperature is reduced as long as the oil velocity at the outer HV oil cooling duct is high enough. When comparing Figs. 7 and 13 it is observed that the location of the hot spot (106 °C (379 K) for the detailed case and 88 °C (361 K) for the variation in HV cooling duct width) is modified when the HV vertical cooling width is varied.

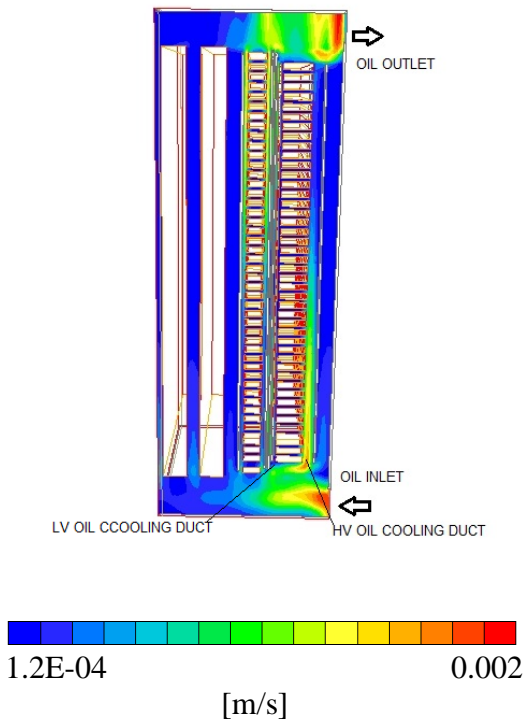


Fig 16 Velocity contour

The velocity contour is shown in Fig. 16. As depicted oil enters at the bottom and raises upwards through the HV oil cooling duct at 0.0015 m/s from disc 1 and then it decreases and mixes with oil from the inner LV cooling duct decelerating at the exit of the HV oil cooling duct. Also, it is observed that oil at relatively high velocity enters the HV outer cooling duct and at a the disc15 it starts to reduce velocity due to the fact that it starts to move in the horizontal cooling ducts.

Then an investigation into the variation in width of the LV cooling duct from 9.525 mm to 29.52 mm was performed and the temperature contour is shown in Fig. 17.

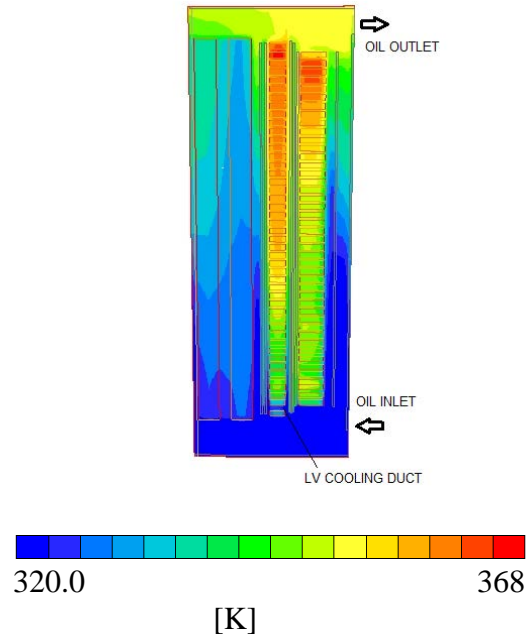


Fig. 17 Temperature contour

As observed in Fig. 17 of variation of LV cooling duct width, the LV winding temperature 95°C (368 K) is higher than the one found with the variation of HV cooling duct width 88 °C(361 K). Also as observed in the same Fig. 17 there is a variation in temperature of the HV winding.

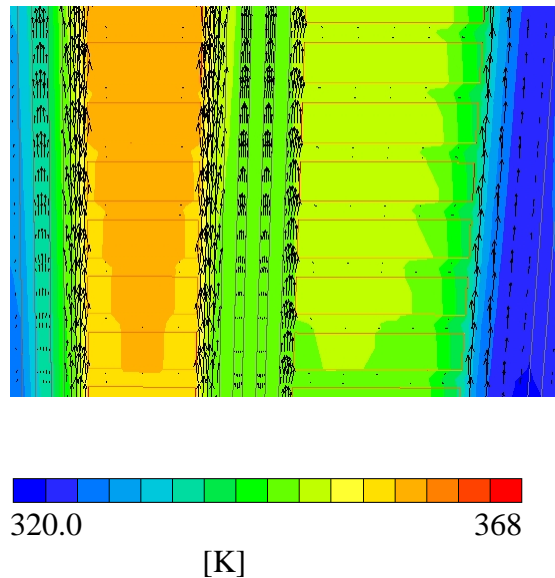


Fig. 18 Temperature close-up

In close up of temperature distribution of HV and LV cooling ducts of Fig. 17 it is shown the oil distribution in the windings. This Fig. 18 shows that there is an decrease in the LV temperature winding due to the increase in the cold cooling oil from the outer LV oil cooling duct as it is observed with the oil temperature of 71 °C (344 K) at the outer and inner LV cooling ducts.

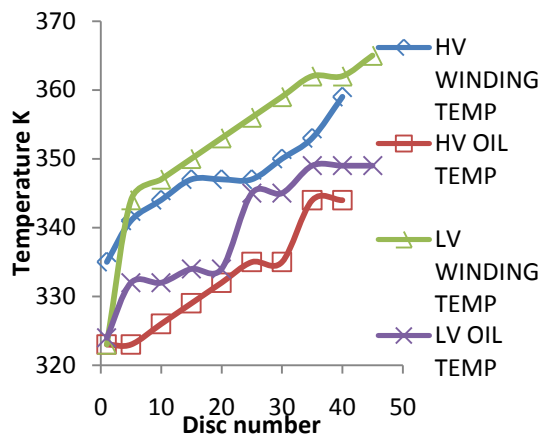


Fig. 19 Centerline temperatures

Fig. 19 shows a graph of the HV oil and winding temperature along the vertical centerline of the HV and LV windings and oil cooling ducts. The oil temperature increases with height but at certain locations it is constant as can be seen between disks 10 to 30 because cold oil at 51 °C (324 K) passes through the outer vertical and horizontal HV cooling ducts absorbing heat from discs and increasing its temperature to 77 °C (350 K). A different effect happens when oil is passing through the inner LV cooling duct. It absorbs heat from the LV discs and heats up to a value of 95 °C (368 K). The velocity contour shown in Fig. 20 depicts velocities in the order of 0.002 and 0.01 m/s which correspond to laminar flow in the cooling ducts of the windings section. Comparing the values previously calculated for the Raleigh numbers the ones obtained are of the same order which are 5.4×10^7 for the high voltage winding and 3.195×10^7 for the low voltage winding

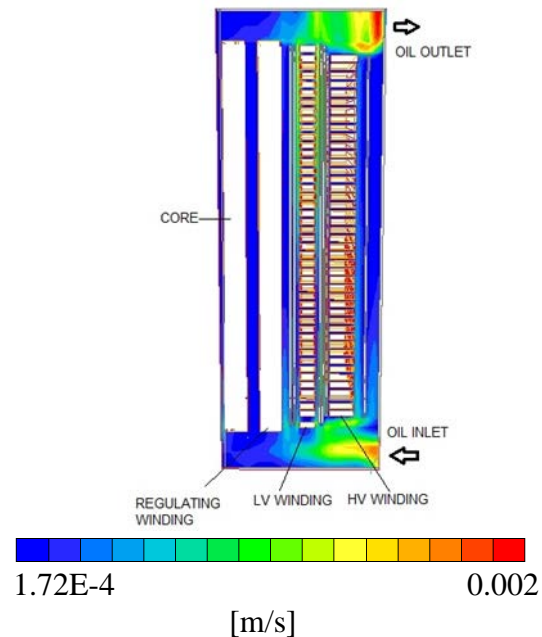


Fig. 20 Velocity contour

7. Conclusions

The simplified CFD model presented includes the most important features of the internal parts of a disc type power transformer. These are the HV, LV and regulating windings as well as the core section, isolators and HV, LV, regulating windings and core oil cooling ducts. Based on the numerical results and heat run test for the power transformer it is concluded that the detailed model compares well with the temperature values obtained from the thermal test. The hot spot value obtained at the top of the detailed model is 100 °C (373 K) and the corresponding one for the heat run test is 101 °C (374 K). Although a more detailed experimental temperature distribution of the windings is needed for the verification of the CFD model the error found based on the heat run test temperatures is 0.26%.

The results show that the variation of HV and LV vertical cooling oil duct width helps to reduce the hot spot in the LV winding section. It was also shown that normally in this direct

cooling design the oil velocities encountered in the horizontal cooling ducts are negligible which does not help the cooling of the discs. The LV and HV oil cooling duct width variation show that oil velocities encountered in the horizontal cooling ducts start to be higher which clearly improve the cooling of the discs. The variation of the HV outer radius shows some improvement in terms of hot spot value. The oil velocities in this arrangement are low but provide enough cold oil to the HV and LV discs. All these variations outlined although difficult to implement as modifications during the design phase of the power transformer may be possible due to the fact that the electromagnetical design may be reviewed as well as the mechanical design of the power transformer. It would be useful if other possible variations in geometric parameters of the power transformer could be investigated such as the number of discs in the HV and LV windings and the heat dissipation of the HV and LV windings.

Acknowledgments

We thank to Consejo Nacional de Ciencia y Tecnología (CONACYT), Instituto de Ingeniería (UNAM) and Industria Eléctrica de México, for the grants, computing facilities and heat run test results provided in order to be able to perform the necessary works for the investigation. We also thank to Eduardo A. Tello, B.Eng. (Aerospace) Dominic Engineering Ltd., Ottawa Canada for his contribution towards the English review of the manuscript.

References

- [1] L.W. Pierce, “ A thermal model for optimized distribution and small power transformer design”, *IEEE Transactions on Power Systems*, vol. 2, no. 2, 1999
- [2] L.W. Pierce, “An investigation of the thermal performance of an oil filled transformer winding”, *IEEE Trans. Power Delivery*, Vol 7, No. 3, pp 1347-1358, July, 1992.
- [3] E.J. Kranenbourg, C.O. Olsson, B.R. Samuelson, L.A. Lundin, R.M. Missing “Numerical study on mixed and thermal streaking in power transformer windings”, 5th Thermal Sciences Conference, The Netherlands, 2008.
- [4] D. Susa, M. Lethonen , H. Nordman, “Dynamic thermal modelling of power transformers”, *IEEE Transactions on Power Delivery*, Vol 20 , pp. 1919-1928, January, 2005.
- [5] T. Talu, “Modelling of thermal processes of a hydraulic cooling system for a power transformer”, *The Scientific Bulletin of Vallarta University, Materials and Mechanics*, No. 6, 2011.
- [6] “ANSI/IEEE Loading Guide for Mineral oil Immersed Transformer”, C57.91-1995, 1996.
- [7] W. Van der Veken, J. Declerk , M. Baelmans, Van Mileghem, “Accurate hot spot modeling in a power transformer leading to improved design and performance”, Presented at IEEE Transmission and Distribution Conference, New Orleans USA, 1999.
- [8] F. Torriano, M. Chaaban, P. Picher, “Numerical study of parameters affecting the temperature distribution in a disc-type transformer winding”, *Applied Thermal Engineering*, Vol 30, pp. 20134-2044, May, 2010.
- [9] M.K. Pradhan, T.S. Ramu, “Prediction of hottest spot temperature (HST) in power and station transformers”, *IEEE Trans. Power Delivery*, 18,(2003), 1275-1283.
- [10] S.V. Patankar, *Numerical Heat Transfer and Fluid Flow*, Ed. New York: Hemisphere, 1980.
- [11] D. Azizi, A. Gholami, “Hot spot temperature analysis in 3 phase Transformers using fem method”, *International Journal of Modern Engineering Research*, vol. 1, issue 2, pp. 425-429, 2011.